Acta Crystallographica Section C
Crystal Structure Communications
ISSN 0108-2701

Comparison of racemic *epi*-inosose and (−)-*epi*-inosose

Shobhana Krishnaswamy,[a]* Madhuri T. Patil[b] and Mysore S. Shashidhar[b]

[a]Centre for Materials Characterization, National Chemical Laboratory, Pune 411 008, India, and [b]Division of Organic Chemistry, National Chemical Laboratory, Pune 411 008, India
Correspondence e-mail: s.krishnaswamy@ncl.res.in

Received 31 August 2011
Accepted 26 September 2011
Online 6 October 2011

The conversion of *myo*-inositol to *epi*-inositol can be achieved by the hydride reduction of an intermediate *epi*-inosose derived from *myo*-inositol. (−)-*epi*-Inosose, (I), crystallized in the monoclinic space group $P2_1$, with two independent molecules in the asymmetric unit [Hosomi *et al.* (2000). *Acta Cryst.* C**56**, e584–e585]. On the other hand, (2*RS*,3*SR*,5*SR*,6*SR*)-*epi*-inosose, $C_6H_{10}O_6$, (II), crystallized in the orthorhombic space group $Pca2_1$. Interestingly, the conformation of the molecules in the two structures is nearly the same, the only difference being the orientation of the C-3 and C-4 hydroxy H atoms. As a result, the molecular organization achieved mainly through strong O—H···O hydrogen bonding in the racemic and homochiral lattices is similar. The compound also follows Wallach's rule, in that the racemic crystals are denser than the optically active form.

Comment

epi-Inositol is known to affect regulation of the *myo*-inositol biosynthetic pathway (Shaldubina *et al.*, 2002) and has been evaluated as a potential antidepressant drug that could interact with the Li^+ ion and *myo*-inositol receptors in the brain (Einat *et al.*, 1998; Belmaker *et al.*, 1998; Williams *et al.*, 2002). We have reported previously the synthesis of *epi*-inositol by the reduction of racemic *epi*-inosose (Patil *et al.*, 2011).

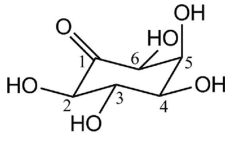

(I) (−)-*epi*-inosose
(II) *rac*-*epi*-inosose

A Cambridge Structural Database (CSD, Version 5.31; Allen, 2002) search yielded the structure of the optically active (−)-*epi*-inosose (CSD refcode XEGVUA; Hosomi *et al.*, 2000) prepared enantioselectively by a bioconversion from *myo*-inositol (Hosomi *et al.*, 2000). We were thus presented with an opportunity for the comparison of the molecular assembly in the crystals of these homochiral, (I), and racemic, (II), inososes. Single-crystal X-ray intensity measurements for

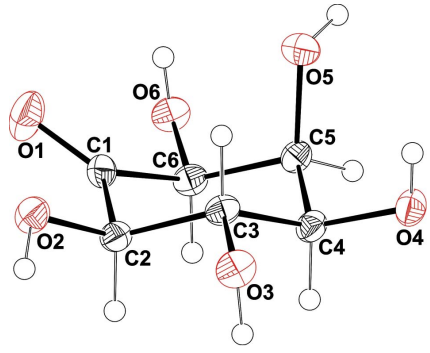

Figure 1
The molecular structure of racemic *epi*-inosose, (II) [the (2*R*,3*S*,5*S*,6*S*)-enantiomer], showing the atom-labelling scheme. Displacement ellipsoids are drawn at the 50% probability level and H atoms are shown as small spheres of arbitrary radii.

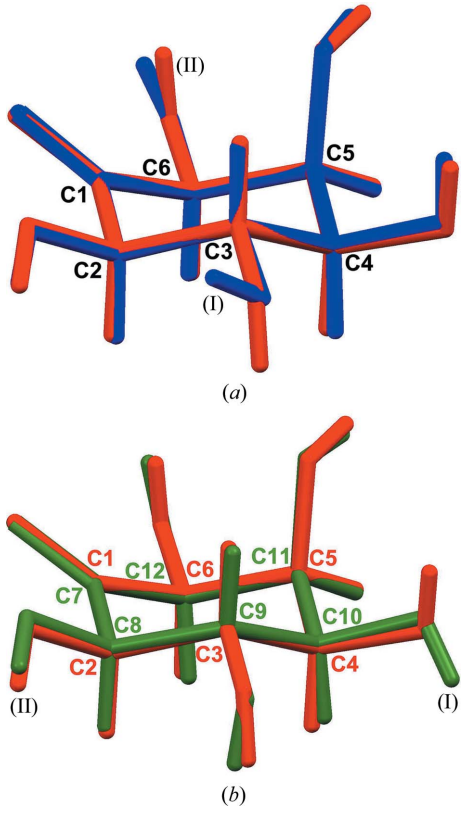

Figure 2
The overlap of the molecules in the crystals of (−)-*epi*-inosose, (I), and racemic *epi*-inosose, (II), showing the differences in the orientations of the hydroxy groups. In (*a*), one of the two independent molecules in the asymmetric unit of (I) (blue in the electronic version of the paper) and the corresponding enantiomer in (II) (red) is shown, while in (*b*) the second independent molecule in the asymmetric unit of (I) (green) and the corresponding enantiomer in (II) (red) is shown.

 doi:10.1107/S0108270111039412

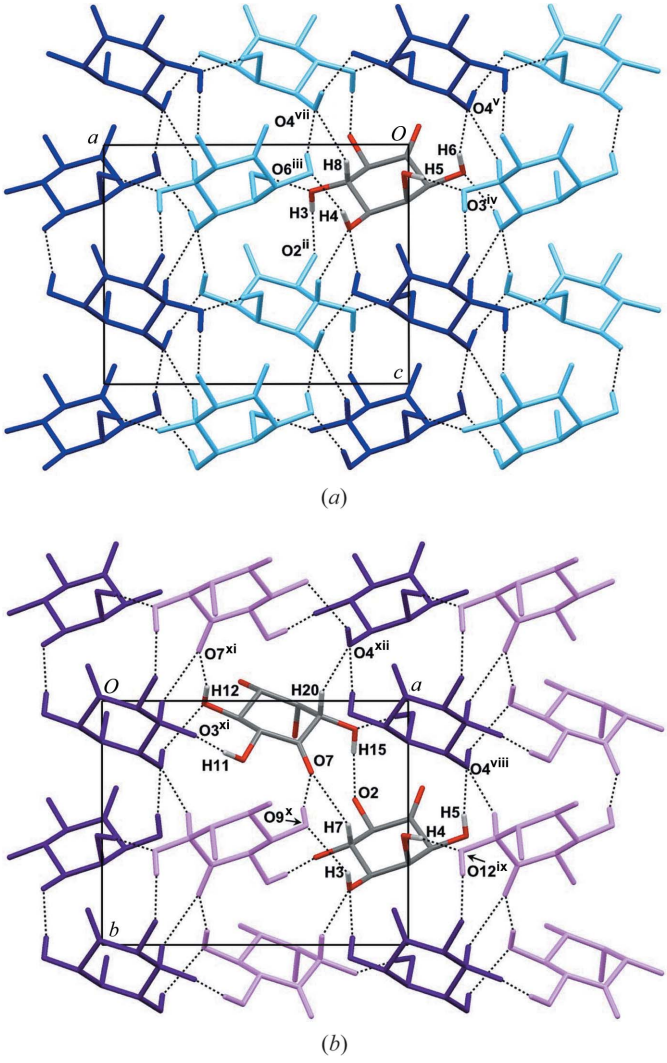

Figure 3
Chains of molecules linked through hydrogen-bonding interactions (dotted lines) in the crystal structures of (*a*) (II) and (*b*) (I). The different colours represent the enantiomers of (II) in (*a*) (dark blue and light blue in the electronic version of the paper) and the independent molecules in the asymmetric unit of (I) in (*b*) (purple and light pink). H atoms not involved in hydrogen bonding have been omitted. [Symmetry codes: (ii) $-x+\frac{1}{2}, y, z+\frac{1}{2}$; (iii) $x+\frac{1}{2}, -y, z$; (iv) $x-\frac{1}{2}, -y, z$; (v) $-x, -y, z-\frac{1}{2}$; (vii) $-x+\frac{1}{2}, y, z-\frac{1}{2}$; (viii) $-x+2, y-\frac{1}{2}, -z$; (ix) $-x+2, y+\frac{1}{2}, -z$; (x) $-x+1, y+\frac{1}{2}, -z$; (xi) $-x+1, y-\frac{1}{2}, -z$; (xii) $x, y-1, z$.]

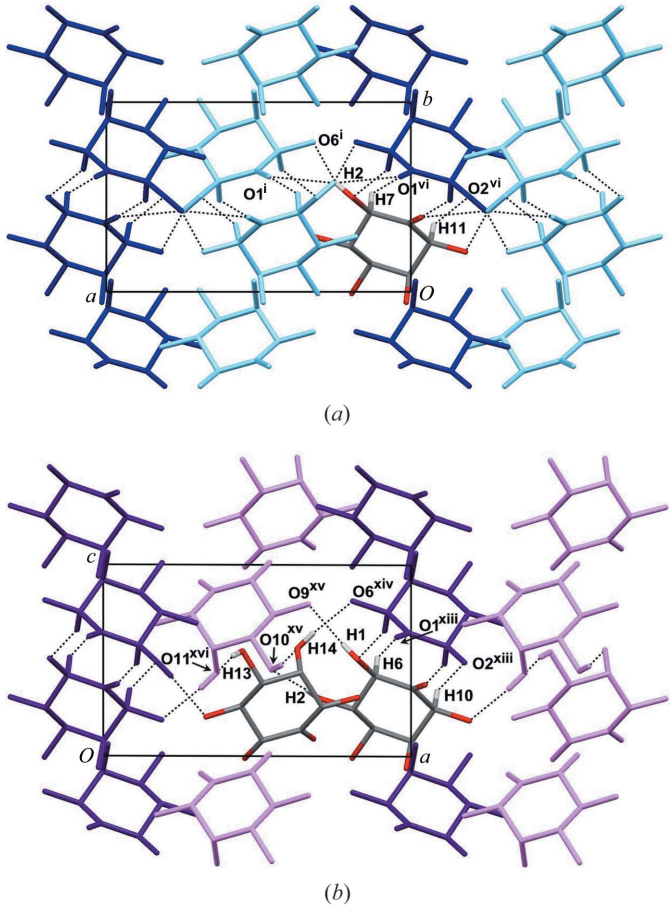

Figure 4
A view of the molecular packing down (*a*) the *c* axis in crystals of (II) and (*b*) the *b* axis in crystals of (I). Dotted lines represent hydrogen-bonding interactions, some of which (shown in Fig. 3) have been omitted for clarity. [Symmetry codes: (i) $x+\frac{1}{2}, -y+1, z$; (vi) $-x, -y+1, z+\frac{1}{2}$; (xiii) $x+2, y+\frac{1}{2}, -z+1$; (xiv) $-x+2, y-\frac{1}{2}, -z+1$; (xv) $-x+1, y+\frac{1}{2}, -z+1$; (xvi) $-x+1, y-\frac{1}{2}, -z+1$.]

crystals of (II) were recorded at ambient temperature (297 K), as reported for (I). Crystals of the racemic ketone are orthorhombic, belonging to the noncentrosymmetric space group $Pca2_1$ (Fig. 1), while the homochiral ketone crystallizes in the noncentrosymmetric space group $P2_1$, with two independent molecules (*A* and *B*) in the asymmetric unit. The atom numbering for the racemic form is consistent with that reported for the optically active compound to enable easier comparison of the crystal structures.

The superimposition of the molecules in the asymmetric unit of (I) and the corresponding enantiomer in (II) reveals an excellent fit of the non-H atoms, with r.m.s. deviations of 0.0058 and 0.0094 Å for the overlaid non-H atoms shown in Figs. 2*a* and 2*b*, respectively. The most significant differences are in the orientations of the hydroxy H atoms at C3 and C4. The conformation of the C3 hydroxy H atom of (II) matches that of molecule *B* in the asymmetric unit of crystals of (I), whereas the conformation of the C4 hydroxy group matches that of molecule *A*.

There is a close correspondence in the unit-cell parameters of the two structures: the *a* axes lengths are nearly the same and interchange of the *b* and *c* axes of the orthorhombic racemic form results in edge lengths that are nearly identical to those of the homochiral crystal lattice [a = 11.197 (2), b = 8.932 (2), c = 6.976 (2) Å and β = 90.21 (2)° for (I)]. In accordance with Wallach's rule (Wallach, 1895; Brock *et al.*, 1991), the racemic crystal is 1.7% denser than the enantiomerically pure crystal, and its melting point is 492–495 K. The melting point of the crystals of (I) is not available for comparison. The unit cell of racemic *epi*-inosose consists of four molecules, *i.e.* two pairs of enantiomers, whereas that of (−)-*epi*-inosose contains two pairs of the two symmetry-independent molecules of the asymmetric unit.

The presence of five hydroxy groups and a carbonyl group results in extensive hydrogen-bonding interactions in the crystal. In the crystals of (II), each enantiomer forms a homochiral hydrogen-bonded chain along the *c* axis through O6—H6···O4^{v}, with adjacent heterochiral molecular chains along the *a* axis linked by short and linear O3—H3···O2^{ii}, O4—H4···O6^{iii}, O5—H5···O3^{iv} and C3—H8···O4^{vii} interactions (Fig. 3*a*, symmetry codes and geometric parameters in Table 1). In the case of (I), each of the two molecules in the asymmetric unit forms a similar O6—H5···O4^{viii} hydrogen-bonded chain along the *b* axis. Interestingly, the carbonyl O atom (O7) of only one of the molecules of (I) (molecule *B*) is involved in O—H···O hydrogen bonding [O9—H12···O7^{xi}; symmetry codes for (I) as in Fig. 3*b*], because of the conformational differences in the hydroxy groups of the two molecules in the asymmetric unit. The adjacent molecular chains along the *a* axis are linked by a large number of hydrogen-bonding interactions (Fig. 3*b*).

A view of these molecular chains down the *c* axis in (II) and *b* axis in (I) shows a corrugated-sheet-like assembly (Fig. 4). Adjacent sheets are linked by bifurcated hydrogen-bonding interactions involving carbonyl atom O1 (O2—H2···O1^{i} and C2—H7···O1^{vi}) and O2—H2···O6^{i} and C6—H11···O2^{vi} contacts in the racemic crystal (Fig. 4*a* and Table 1). In the crystals of the optically active form, neighbouring sheets are linked by O2—H1···O9^{xv}, O3—H2···O10^{xv}, O10—H13···O11^{xvi}, O11—H14···O6^{xiv}, C2—H6···O1^{xiii} and C6—H10···O2^{xiii} contacts (Fig. 4*b*). Thus, the overall molecular organization in the crystals of the racemic and enantiopure compound is remarkably similar. This is primarily due to the fact that the second molecule in the asymmetric unit of (I) plays the role of the second enantiomer in the crystal packing. While the thermodynamic stability of the two crystals cannot be experimentally evaluated owing to the absence of adequate thermal data, estimation of lattice energies for (I) and (II) using the *Oprop* module of the *OPiX* program suite (Gavezzotti, 2003) yielded a value of −204.75 kJ mol^{-1} for (I) and −253.5 kJ mol^{-1} for (II), consistent with the crystal densities.

Experimental

Racemic *epi*-inosose, (II), was synthesized as reported previously (Patil *et al.*, 2011). Prism-shaped crystals (m.p. 492–495 K) were obtained by slow evaporation from a solution in hot water.

Crystal data

$C_6H_{10}O_6$
M_r = 178.14
Orthorhombic, $Pca2_1$
a = 11.1825 (18) Å
b = 6.9752 (12) Å
c = 8.7930 (15) Å
V = 685.9 (2) Å^3
Z = 4
Mo $K\alpha$ radiation
μ = 0.16 mm^{-1}
T = 297 K
0.29 × 0.29 × 0.17 mm

Data collection

Bruker SMART APEX CCD area-detector diffractometer
Absorption correction: multi-scan (*SADABS*; Bruker, 2003)
T_{min} = 0.956, T_{max} = 0.974
3225 measured reflections
653 independent reflections
647 reflections with $I > 2\sigma(I)$
R_{int} = 0.016

Table 1
Hydrogen-bond geometry in (II) (Å, °).

D—H···A	D—H	H···A	D···A	D—H···A
O2—H2···O1^{i}	0.85 (4)	2.57 (4)	3.191 (2)	131 (3)
O2—H2···O6^{i}	0.85 (4)	2.02 (4)	2.833 (2)	159 (4)
O3—H3···O2^{ii}	0.87 (4)	1.93 (4)	2.791 (3)	172 (4)
O4—H4···O6^{iii}	0.78 (4)	2.10 (4)	2.844 (2)	161 (3)
O5—H5···O3^{iv}	0.91 (3)	1.92 (3)	2.822 (2)	171 (2)
O6—H6···O4^{v}	0.79 (3)	2.01 (4)	2.760 (2)	160 (3)
C2—H7···O1^{vi}	0.98	2.52	3.374 (3)	145
C3—H8···O4^{vii}	0.98	2.52	3.422 (3)	152
C6—H11···O2^{vi}	0.98	2.49	3.392 (3)	154

Symmetry codes: (i) $x+\frac{1}{2}, -y+1, z$; (ii) $-x+\frac{1}{2}, y, z+\frac{1}{2}$; (iii) $x+\frac{1}{2}, -y, z$; (iv) $x-\frac{1}{2}, -y, z$; (v) $-x, -y, z-\frac{1}{2}$; (vi) $-x, -y+1, z+\frac{1}{2}$; (vii) $-x+\frac{1}{2}, y, z-\frac{1}{2}$.

Refinement

$R[F^2 > 2\sigma(F^2)]$ = 0.026
$wR(F^2)$ = 0.068
S = 1.15
653 reflections
129 parameters
1 restraint
H atoms treated by a mixture of independent and constrained refinement
$\Delta\rho_{max}$ = 0.25 e Å^{-3}
$\Delta\rho_{min}$ = −0.13 e Å^{-3}

All inositol ring H atoms were placed in geometrically idealized positions, with C—H = 0.98 Å. They were constrained to ride on their parent atoms, with U_{iso}(H) = 1.2U_{eq}(C). The O-bound H atoms were located in difference Fourier maps and refined isotropically. The refined O—H distances were in the range 0.79 (3)–0.91 (3) Å. Although (I) is racemic, it crystallizes in a noncentrosymmetric space group. In the absence of strong anomalously scattering elements in the structure, the absolute structure was chosen arbitrarily and the Friedel pairs were merged prior to structure refinement.

Data collection: *SMART* (Bruker, 2003); cell refinement: *SAINT* (Bruker, 2003); data reduction: *SAINT*; program(s) used to solve structure: *SHELXS97* (Sheldrick, 2008); program(s) used to refine structure: *SHELXL97* (Sheldrick, 2008); molecular graphics: *ORTEP-3* (Farrugia, 1997) and *Mercury* (Macrae *et al.*, 2006); software used to prepare material for publication: *SHELXTL* (Sheldrick, 2008) and *PLATON* (Spek, 2009).

SK and MTP are recipients of Senior Research Fellowships from CSIR, New Delhi, India. This work was supported by the Department of Science and Technology, New Delhi, India.

Supplementary data for this paper are available from the IUCr electronic archives (Reference: SF3158). Services for accessing these data are described at the back of the journal.

References

Allen, F. H. (2002). *Acta Cryst.* B**58**, 380–388.
Belmaker, R. H., Agam, G., Van Calker, D., Richards, M. H. & Kofman, O. (1998). *Neuropsychopharmacology*, **19**, 220–232.
Brock, C. P., Schweizer, W. B. & Dunitz, J. D. (1991). *J. Am. Chem. Soc.* **113**, 9811–9820.
Bruker (2003). *SADABS* (Version 2.05), *SMART* (Version 5.631) and *SAINT* (Version 6.45). Bruker AXS Inc., Madison, Wisconsin, USA.
Einat, H., Elkabaz-Shwortz, Z., Cohen, H., Kofman, O. & Belmaker, R. H. (1998). *Int. J. Neuropsychopharmacol.* **1**, 31–34.
Farrugia, L. J. (1997). *J. Appl. Cryst.* **30**, 565.
Gavezzotti, A. (2003). *OPiX*. University of Milan, Italy.

Hosomi, H., Ohba, S., Ogawa, S. & Takahashi, A. (2000). *Acta Cryst.* C**56**, e584–e585.
Macrae, C. F., Edgington, P. R., McCabe, P., Pidcock, E., Shields, G. P., Taylor, R., Towler, M. & van de Streek, J. (2006). *J. Appl. Cryst.* **39**, 453–457.
Patil, M. T., Krishnaswamy, S., Sarmah, M. P. & Shashidhar, M. S. (2011). *Tetrahedron Lett.* **52**, 3756–3758.
Shaldubina, A., Ju, S., Vaden, D. L., Ding, D., Belmaker, R. H. & Greenberg, M. L. (2002). *Mol. Psychiatry*, **7**, 174–180.
Sheldrick, G. M. (2008). *Acta Cryst.* A**64**, 112–122.
Spek, A. L. (2009). *Acta Cryst.* D**65**, 148–155.
Wallach, O. (1895). *Liebigs Ann. Chem.* **286**, 90–143.
Williams, R. S., Cheng, L., Mudge, A. W. & Harwood, A. J. (2002). *Nature (London)*, **417**, 292–295.